MULTI-PASS ERS-ENVISAT CROSS-INTERFEROMETRY METHODS AND RESULTS

Urs Wegmüller, Charles Werner, Othmar Frey, Tazio Strozzi, and Maurizio Santoro

Gamma Remote Sensing AG, Worbstrasse 225, CH-3073 Gümligen, Switzerland,
http://www.gamma-rs.ch, wegmuller@gamma-rs.ch

ABSTRACT

ERS-ENVISAT Tandem (EET) cross-interferometry (CInSAR) pairs are characterized by long 2km baselines and short 28 minute time intervals [1]. Over some sites multiple pairs are available. In our work we discuss multi-pass interferometric techniques and investigate for several applications, including DEM generation, mapping of fast motions and grounding line mapping for Antarctic ice sheets, the use of multiple EET pairs.

1. INTRODUCTION

Multi-pass differential interferometry was successfully used for a variety of applications using data of different orbital SAR sensors. Now, thanks to the dedicated ERS – ENVISAT Tandem campaigns, plenty of EET pairs with suited baselines for CInSAR are available in the archives, including in many cases also multiple EET pairs acquired in the same track. Using such data we investigated the potential of multi-pass EET CInSAR for several applications.

In Section 2 we review the INSAR phase model. In Section 3 multi-pass DINSAR techniques using EET pairs is discussed with respect to DEM generation, glacier motion mapping and grounding line detection. Then in Sections 4 to 6 specific cases in these applications are discussed, followed by the conclusions in Section 7.

2. INSAR PHASE MODEL

The unwrapped phase ϕ_{unw} of an interferogram can be expressed as a sum of a topography related term ϕ_{topo}, a displacement term ϕ_{disp}, a path delay term ϕ_{path}, and a phase noise (or decorrelation) term ϕ_{noise}:

$$\phi_{unw} = \phi_{topo} + \phi_{disp} + \phi_{path} + \phi_{noise} \quad (1)$$

The relation between a change in the topographic height σ_h and the corresponding changes in the interferometric phase σ_ϕ is given by,

$$\sigma_h = \frac{\lambda r_1 \sin\theta}{4\pi B_\perp}\sigma_\phi . \quad (2)$$

For the ERS and ENVISAT SAR sensors, with wavelengths around 5.66cm, a nominal incidence angle of 23 degrees, and a nominal slant range of 853 km Equation (2) reduces to

$$\sigma_h \approx 1500\frac{\sigma_\phi}{B_\perp[m]}, \quad (3)$$

allowing to estimate the effect of the topography.
The displacement term, ϕ_{disp}, is related to the coherent displacement of the scattering centers along the radar look vector, r_{disp}:

$$\phi_{disp} = 2kr_{disp} \quad (4)$$

where k is the wavenumber. Here coherent means that the same displacement is observed for adjacent scatter elements.

Changes in the effective path length between the SAR and the surface elements as a result of changing permittivity of the atmosphere, caused by changes in the atmospheric conditions (mainly water vapor), lead to non-zero ϕ_{path}.

Finally, random (or incoherent) displacement of the scattering centers as well as noise introduced by SAR signal noise is the source of ϕ_{noise}. The standard deviation of the phase noise σ_ϕ (reached asymptotically for large number of looks N) is a function of the degree of coherence, γ [2],

$$\sigma_\phi = \frac{1}{2N}\frac{\sqrt{1-\gamma^2}}{\gamma} . \quad (5)$$

Multi-looking and filtering allow to reduce phase noise. The main problem of high phase noise is not so much the statistical error introduced in the estimation of ϕ_{topo} and ϕ_{disp} but the problems it causes with the unwrapping of the *wrapped* interferometric phase.

Most of the time SAR interferometry is used to derive either a DEM or to map the line-of-sight ground deformation. Accordingly the topographic phase ϕ_{topo}, and the displacement phase ϕ_{disp} are the targeted terms in Eq. 1 and the other two terms are considered the error terms.

Proc. 'Fringe 2011 Workshop', Frascati, Italy,
19–23 September 2011 (ESA SP-697, January 2012)

Since the availability of the SRTM DEM, mainly 2-pass differential interferometry is used to derive displacement maps. The topographic phase is simulated based on an existing DEM (e.g. SRTM) and subtracted resulting in a differential interferogram with the displacement phase as the main signal term and the path delay, noise and topographic phase error as the error terms.

Multi-pass differential interferometry is mainly used if no accurate enough DEM is available. The basic idea is that under the assumption of uniform motions having two or more independent observations permits solving for the two unknowns, the topographic height and a LOS displacement rate. Hereby, deriving the topographic height and the LOS displacement rate from the unwrapped phase is not the main difficulty, but to get unwrapped phases for the two interferograms.

An often used strategy to solve the unwrapping problem is to combine the two interferograms into a differential interferogram with less phase variation which is then easier to unwrap. Different approaches are chosen depending on the capability to unwrap one of the interferograms [2]. If unwrapping is not possible, scaling of the phase of the complex valued interferograms with integer factors is still possible. Subtracting pairs with identical intervals permits to eliminate uniform deformation phase. As another example a pair with a 205m baseline and one with a 100m baseline can be combined into a pair with an effective baseline of 5m. Consequently, there will be very little topographic phase in this combined interferogram.

3. MULTI-PASS EET DINSAR

Multi-pass DINSAR techniques are also of interest for EET CInSAR pairs. What is particular with the EET CInSAR pairs is that they all have the same short 28 minute repeat interval and very long baselines between about 1400m and 2600m. As a consequence displacement phase is only present for very fast movements (in the cm/hour order). On the other hand the topographic phase is very sensitive to the terrain elevation with ambiguity heights between about 3m and 7m.

3.1. DEM generation

EET CInSAR is well suited for the generation of DEMs in quite flat areas [1]. The main error source in the EET DEMs is the atmospheric path delay. This error can be reduced statistically by considering multiple EET pairs. Consequently, often multiple EET pairs are used to generate a DEM. The most difficult processing step is the phase unwrapping. Having multiple EET pairs available it is possible to also consider combined interferograms with shorter effective baselines which may help solving the phase unwrapping.

To get a combined interferogram with a shorter effective baseline one complex EET interferogram is multiplied with complex conjugate of the another one. The phase of the combined interferogram corresponds to the phase difference between the two interferogram. Accordingly the effective baseline is the difference between the baselines of the first and second EET pairs. For pairs with 2200m and 1800m baselines the effective baseline of the combined interferogram is 400m. Abrupt elevation changes by about 10m may result in unwrapping errors for the EET pairs with about 5m height ambiguity. With the 400m baseline the height ambiguity is around 24m which reduces the unwrapping problems for a 10m elevation step. The height derived for the combined interferogram can then be used to guide the unwrapping of the initial EET pairs. A specific example will be presented in Section 4.

Another reason to consider a combined EET interferogram is that deformation phase can be eliminated over uniformly moving surfaces. Over the 28 minutes of the acquisition of an EET pair a fast moving glacier can move in the cm range which will result in a significant displacement phase. Considering in a combined interferogram the phase difference between two EET pairs, this displacement phase is eliminated, permitting to derive the elevation on the glacier. Elevations over glaciers and even more so their temporal change, are of high interest as climate indicators and as input for mass balance calculations. A specific example will be presented in Section 5.

3.2. Glacier motion mapping

Initially one of our main objectives for the use of multi-pass EET CInSAR techniques was to map the flow rate of fast moving glaciers.

We were not successful in this mainly because the baselines of the EET pairs acquired in repeat-tracks were too similar to each other. With a 2200m and a 2000m pair we can calculate a combined interferogram with and effective baseline of 200m and derive the topographic height from it. To use this for the simulation of the topographic phase of the 2000m pair is critical because it scales the errors by a factor of 10. For a typical atmospheric path delay error of $\pi/2$ this results in an error of 2.5 phase cycles which is clearly not acceptable for signals up to one phase cycle.

3.3. Grounding line detection

The flow of a glacier, as considered in the previous section, is quite uniform. Tidal motion of shelf ice, on

the other is more or less periodic. Different EET pairs observe different parts of the tidal cycle. Consequently, the line-of-sight displacement phase of multiple EET pairs varies significantly. Combined EET interferogram can be used to strongly reduce the topographic phase as well as uniform motion phase. At the same time the resulting combined tidal phase may remain significant. Ideally, pairs with almost identical baselines are used to eliminate the topographic phase as much as possible. Furthermore, the pairs selected shall ideally catch intervals with significantly differing tidal motion (e.g. one pair during upward and one during downward motion). The tidal motion phase is then substantial. With a time between low and high tide of around 6 hours and assuming 1.2m peak to peak elevation change the average vertical displacement in an 28 minute interval (EET acquisition interval) is still 10cm which will cause more than 3 fringes of deformation phase. A specific example will be presented in Section 6.

4. DEM GENERATION OVER PO VALLEY

For parts of the Po Valley we generated a DEM based on 4 suited EET pairs (see Table 1). The differential interferograms considered are relative to a constant height. The critical processing step is the unwrapping of the interferometric phase. As can be seen in Figure 1, the high phase to height sensitivity with ambiguity heights between about 4m and 7m introduces high phase gradients and phase steps even in overall very flat terrain. This is obvious along the Po river and to the North East where the topography is affected by erosion gullies. For some of these quite local terrain features the unwrapping tends to fail. And sometimes even an operator cannot easily fix the unwrapping.

Based on the 4 EET pairs it is possible to calculate a large number of combined interferograms. We selected four combined interferograms with effective baselines between 280m and 525m as shown in Table 2. Shorter baselines are not well suited for its low height sensitivity. An example of a combined interferogram is shown in Figure 2. Unwrapping with a minimum cost-flow algorithm did not show any obvious errors. Through the complex combination of two differential interferograms the phase noise is higher in the combined interferogram. Areas with very low coherence levels were masked from the solution.

The phase was unwrapped for all the 4 selected combined interferograms. The corresponding height maps were averaged to get an optimized DEM based on the combined interferograms. This DEM was then used to guide the unwrapping of the 4 original EET cross-interferograms. To get the final DEM the 4 individual EET DEMs were combined, permitting to reduce the atmospheric errors to a standard error around 1 meter.

Table 1: EET CInSAR parameters of pairs selected over the Po Valley Indicated are the track number, date, perpendicular baseline component, $B_\perp$, and the Doppler Centroid difference, dDC.

track	date	$B_\perp$[m]	dDC[Hz]
165	*20071006*	*1760*	*754*
165	*20071215*	*1398*	*699*
165	*20080223*	*1674*	*359*
165	*20090207*	*2203*	*861*

Table 2: Effective baselines of combined EET CInSAR pairs selected over the Po Valley.

date1	date2	$B_\perp$[m]
20071215	*20071006*	*360*
20071215	*20080223*	*280*
20090207	*20071006*	*445*
20090207	*20080223*	*525*

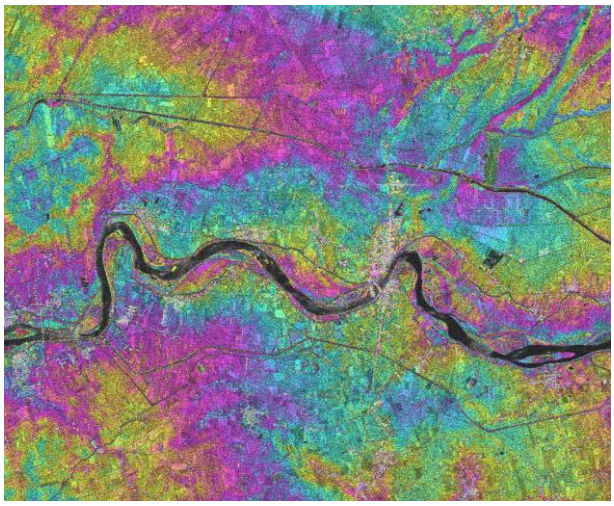

Figure 1 Po Valley, Italy. EET cross-interferogram relative to a constant reference height, track 165, 6-Oct-2007, dt 28min., $B_\perp$ 1760m.

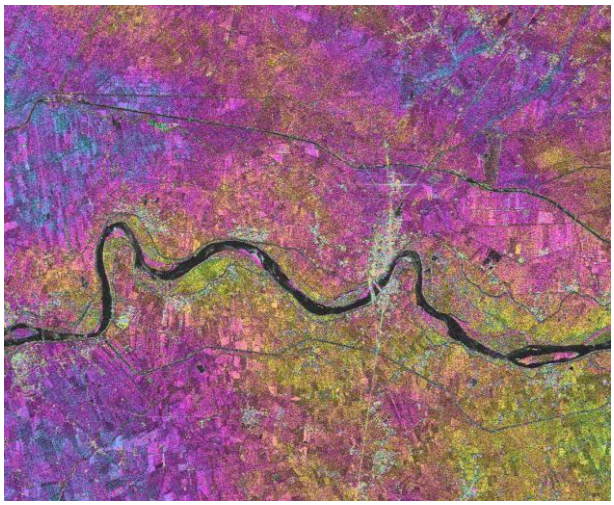

Figure 2 Po Valley, Italy. Combined EET cross-interferogram based on EET pairs on 15-Dec-2007 and 6-Oct-2007 with an effective $B_\perp$ 360m.

5. MULTI-PASS EET CINSAR OVER FAST GLACIERS IN WEST ANTARCTICA

To assess the potential of multi-pass EET cross-interferometry over fast glaciers (this section) and ice sheets (Section 6) we considered two suited pairs over West Antarctica acquired during the dedicated Antarctica EET campaign in 2010 (see Table 3). Based on the two EET pairs a combined interferogram was calculated (see Table 4).

For two sections over land the two EET cross-interferograms and the combined interferogram are shown in Figure 3. For the combined interferogram the height sensitivity is reduced (shorter baseline) and there is no deformation phase for uniform motion. As a consequence, it is possible to derive the topography even on top of fast moving glaciers. Mapping the glacier motion with these data was not successful though, for the reasons discussed in Section 3.2.

6. GROUNDING-LINE MAPPING FOR LARSEN B ICE SHELF

The EET pairs introduced in Section 5 were used to assess the potential of multi-pass EET cross-interferometry for grounding line mapping for the Larsen B Ice Shelf. Let us first consider a small area (4km x 11.2km) which includes floating shelf ice affected by tidal motion in the south and grounded glacier ice in the north. An ERS-1/2 differential interferogram ($B_\perp$ 335m) acquired on 16/17 Nov. 1995 (Figure 4a) is shown together with EET cross-interferograms on 26-Feb-2010 (4b) and 2-Apr-2010 (c), and the combined EET interferogram (Table 4, Figure 4d). An approximate grounding line was drawn in black. For the ERS-1/2 Tandem pair we count north of the grounding line 3 cycles of topographic phase and south of the grounding line 12 cycles of tidal phase. In this case the phase slope changes its sign at the grounding line which facilitates the mapping of the grounding line. For the Feb. 2010 EET interferogram we count 24 cycles of topographic phase and about 4 tidal phase cycles, and for the Apr. 2010 EET pair 20 cycles of topographic phase and about 12 tidal phase cycles, each time with a change in the sign of the phase gradient at the grounding line. The topographic phases observed are consistent with the different baselines, respectively height sensitivities of the different pairs.

Table 3: EET CInSAR parameters of pairs selected over West Antarctica and Larsen B ice shelf. Indicated are the track number, date, perpendicular baseline component, $B_\perp$, and the Doppler Centroid difference, dDC.

track	date	$B_\perp$[m]	dDC[Hz]
152	*20100226*	*2267*	*500*
152	*20100402*	*1940*	*380*

Table 4: Effective baseline of combined EET CInSAR interferogram over West Antarctica and Larsen B ice shelf.

date1	date2	$B_\perp$[m]
20100226	*20100402*	*327*

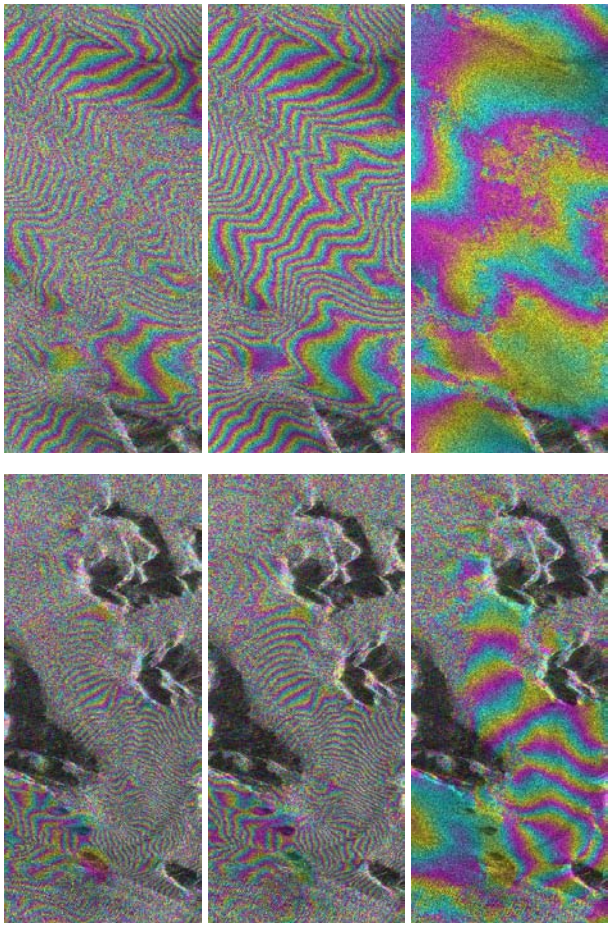

26.2.10, 2267m 2.4.10, 1940m combi, 327m

Figure 3 EET cross-interferograms and combined interferograms over two sections in West Antarctica. Below the image the date and perpendicular baseline is indicated.

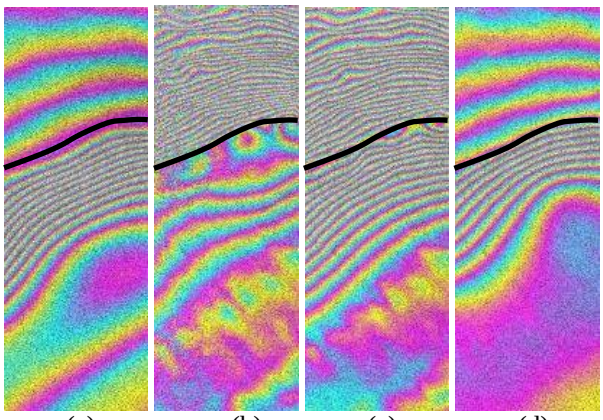

(a) (b) (c) (d)

Figure 4 Four interferograms over West Antarctica. (a) ERS-1/2 on 16/17 Nov. 1995, $B_\perp$ 335m. (b) EET 26. Feb. 2010, $B_\perp$ 2267m. (c) EET 2-Apr-2010, $B_\perp$ 1940m. (d) combined interferogram for EET pairs shown in (b) and (c) with a resulting effective baseline of 327m. The black line indicates the estimated grounding line position.

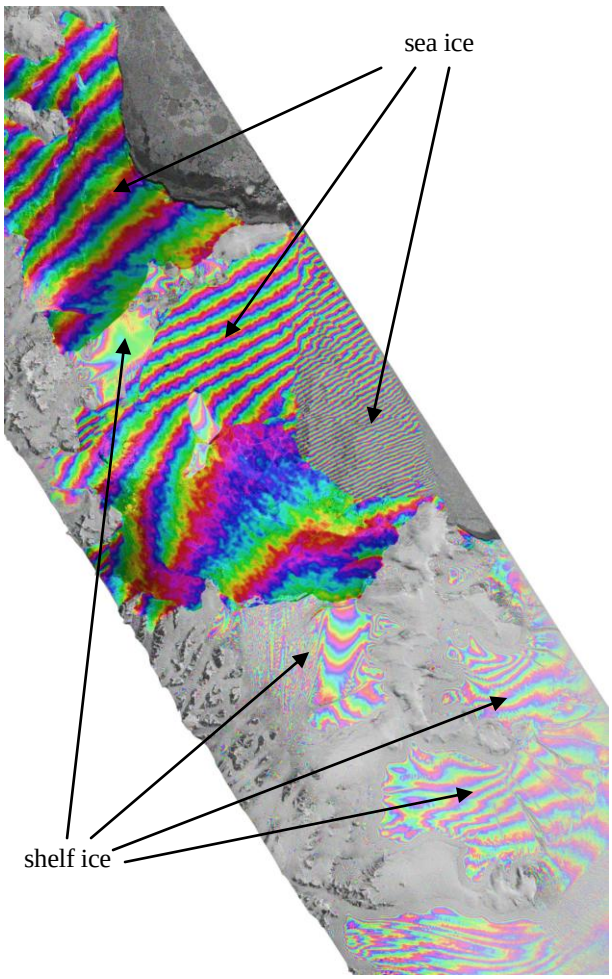

Figure 5 West Antarctica with Larsen B ice shelf. EET Cross-Interferogram 2-Apr-2010, $B_\perp$ 1940m.

In the combined interferogram (4d) about 4 topographic phase cycles are observed north of the grounding line and about 8 tidal phase cycles south of it. It is unfortunate that the sign of the phase gradient does not change at the grounding line. Furthermore, the effective baseline is not very short which makes the separation of tidal and topographic phase difficult. So in this particular case considering the individual EET pairs in addition to the combined interferogram is recommended for the mapping of the grounding line.

Figure 5 shows the April 2010 EET pair and Figure 6 the combined interferogram over a much larger area. In some areas the grounding line can be determined in other areas this seems difficult because of too high phase gradients in the case of the long baseline EET pair which make it almost impossible to locate the location where the sign of the phase slope changes. In the combined interferogram the phase over the shelf ice does not show high variations except for the tidal phase near the grounding line. To precisely locate the grounding line in the combined interferogram is

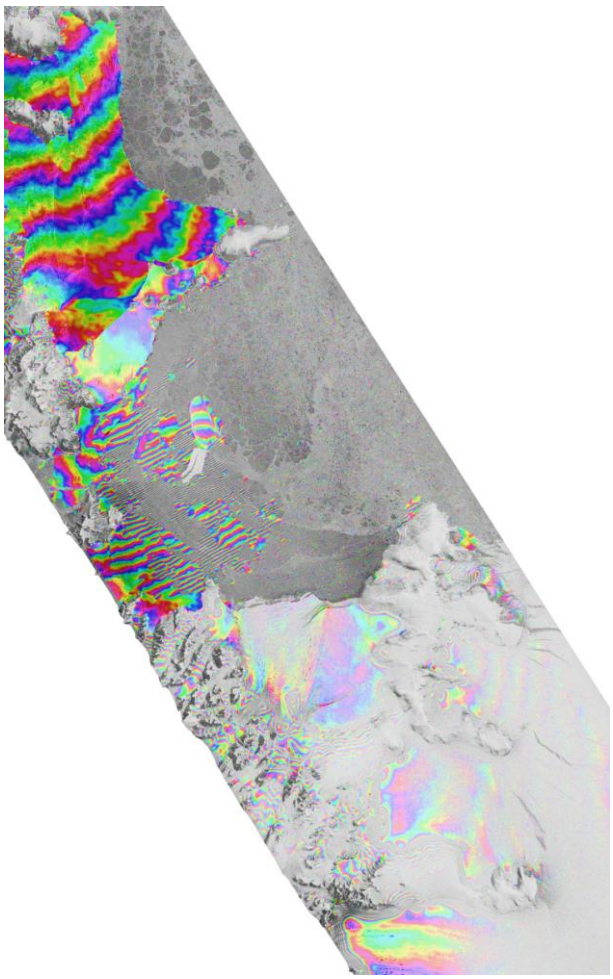

Figure 6 West Antarctica with Larsen B ice shelf. EET combined interferogram 26-Feb-2010 and 2-Apr-2010, $B_\perp$ 327m.

difficult though because tidal and topographic phase is often confused. Furthermore, in the Feb. 2010 EET pair the coherence is very low over parts of the shelf ice, which also prevents in these areas from an interpretation of the combined phase.

7. CONCLUSIONS

One important EET CInSAR application is the generation of DEMs over relatively flat areas. Having multiple pairs permits improving the accuracy of the DEMs generated. The main error, the atmospheric path delay, does typically not correlate between multiple pairs, so that better accuracies can be achieved by combining multiple pairs. In EET CInSAR phase unwrapping is not trivial even in rather flat areas because of the high phase to elevation sensitivity with height ambiguities around 5 meter. Having multiple pairs with different baselines available helps with the phase unwrapping. Apart from the EET pairs, combinations can be considered. Combinations with a shorter baseline can more easily be unwrapped, which helps avoiding unwrapping errors. Considering multiple EET pairs makes the DEM generation more robust and more accurate results are achieved.

In the case of fast moving glaciers, considering multiple EET pairs was used to derive the topography over large glaciers, but we could not accurately estimate the glacier velocity. The effective baselines of the combined interferogram without displacement phase are typically much shorter than the 2km EET baselines. This facilitates phase unwrapping, but up-scaling of the resulting topographic phase to a long EET baseline is not accurate enough to fully compensate the topographic phase of the 2km baseline pair.

Over ice sheets with tidal motion the tidal phase of different EET pairs usually differs because of the tidal cycle. An advantage of the combined interferogram is that the topographic phase is much reduced. In ideal combinations, the combined interferogram will show many tidal phase cycles (>5) but not too much topographic phase which makes the mapping of the grounding line quite easy. It is furthermore an advantage if the phase slope changes the sign at the grounding line. In the combination we investigated, the effective baseline was quite long (> 300m) the combined period showed about 5 tidal phase cycle, but the phase slope did not change the sign at the grounding line. Therefore, the grounding line mapping remained difficult and was only partly possible.

8. Acknowledgments

This work was supported by ESA under contract 22526/09/I-LG on ERS-ENVISAT Tandem Cross-Interferometry Campaigns: Case Studies. ERS and ASAR data copyright ESA (CAT 6744).

9. REFERENCES

[1] Wegmüller U., M. Santoro, C. Werner, T. Strozzi, A. Wiesmann, and W. Lengert, “DEM generation using ERS–ENVISAT interferometry“, Journal of Applied Geophysics Vol. 69, pp 51–58, 2009, doi:10.1016/j.jappgeo.2009.04.002.

[2] Wegmüller U., and T. Strozzi, Characterization of differential interferometry approaches, EUSAR'98, 25-27 May, Friedrichshafen, Germany, VDE-Verlag, ISBN 3-8007-2359-X, pp. 237-240, 1998.